

Lattice exciton-polaron problem by quantum Monte Carlo simulations

Martin Hohenadler,^{1,*} Peter B. Littlewood,¹ and Holger Fehske²

¹*Theory of Condensed Matter, Cavendish Laboratory, University of Cambridge, Cambridge CB3 0HE, United Kingdom*

²*Institute of Physics, Ernst-Moritz-Arndt University Greifswald, 17487 Greifswald, Germany*

Exciton-polaron formation in one-dimensional lattice models with short- or long-range carrier-phonon interaction is studied by quantum Monte Carlo simulations. Depending on the relative sign of electron and hole-phonon coupling, the exciton-polaron size increases or decreases with increasing interaction strength. Quantum phonon fluctuations determine the (exciton-) polaron size and yield translation-invariant states at all finite couplings.

PACS numbers: 71.35.-y, 02.70.Ss, 63.20.Ls, 71.38.-k

I. INTRODUCTION

The binding of electron-hole (E-H) excitations into excitons (Xs), governing the optical properties of most nonmetallic materials,¹ plays a major role in, e.g., organics,² nanostructure devices,³ quantum light sources,⁴ Bose-Einstein condensation⁵ and DNA.⁶

The coupling of Xs to phonons is widely relevant,^{7,8} and gives rise to exciton-polaron (X-P) formation, corresponding to quasiparticles consisting of an E-H pair and a virtual phonon cloud. Apart from the essential role of phonons in relaxation processes after optical excitation, lattice-coupling alters the X radius which determines, e.g., the oscillator strength in optics and the overlap of X wave functions required for Bose-Einstein condensation. Very recently, a direct observation of an exciton-polaron in photoluminescence spectra of quantum dots has been reported.⁹

Examples where X-Ps of intermediate size are clearly implicated in current experiments include transition metal oxides, such as insulating manganites¹⁰ and nickelates,^{11,12} though the situation in cuprates is controversial.^{11,13} Another important class of materials is conjugated polymers (e.g., Ref. 14). In these systems, the well-known approximations of small Frenkel or large Wannier-Mott Xs are unjustified, requiring nonperturbative theories which includes relative E-H motion.¹⁴

Polaron formation is a complex, nonlinear, many-body problem which cannot be completely described by renormalization of effective masses.¹⁵ In particular, the quantum nature of phonons—leading to retarded (self-)interaction—has to be taken into account. Since polaron physics is governed by lattice dynamics on the unit-cell scale, the discrete nature of the crystal cannot be neglected.¹⁶

The resulting problem of an interacting E-H pair with coupling to quantum phonons represents a long-standing open question in condensed matter physics. Whereas some exact results are available without phonons,^{17,18} standard methods such as perturbation theory, and variational or adiabatic approximations^{19,20,21,22,23} are often of uncertain reliability. Furthermore, computational approaches are very demanding, and we are not aware of any exact results for quantum phonons.

Here we present unbiased numerical results for the quantum lattice X-P within a simple E-H model, obtained by means

of quantum Monte Carlo (QMC) simulations. This method, well established in the field of polaron physics, treats all couplings on the same footing and is not restricted to a specific X size or parameter region. Our model study of several different Hamiltonians yields important results for the effects of carrier-phonon interaction on X properties.

II. MODEL

Extending previous work,^{17,24,25} we consider a simple model in one dimension (1D) defined by the Hamiltonian

$$H = -t_e \sum_{\langle i,j \rangle} e_i^\dagger e_j - t_h \sum_{\langle i,j \rangle} h_i^\dagger h_j - \sum_{ij} u_{ij} \hat{n}_{i,e} \hat{n}_{j,h} \quad (1)$$

$$+ \frac{\omega_0}{2} \sum_i (\hat{x}_i^2 + \hat{p}_i^2) - \sum_{i,j} f_{j,i} \hat{x}_j (\alpha_e \hat{n}_{i,e} + \alpha_h \hat{n}_{i,h})$$

with long-range Coulomb attraction

$$u_{ij} = \begin{cases} U_0 & , \quad i = j, \\ U_1/|i-j| & , \quad i \neq j \end{cases} \quad (2)$$

where $U_0 > U_1 > 0$ (i.e., attractive interaction), and long-range carrier-phonon interaction

$$f_{j,i} = \frac{1}{(|j-i|^2 + 1)^{3/2}}. \quad (3)$$

Here e_i^\dagger (h_i^\dagger) creates an E (H) at site i , and \hat{x}_i (\hat{p}_i) denotes the displacement (momentum) of a harmonic oscillator at site i . The fermionic density operators are defined as $\hat{n}_{i,e} = e_i^\dagger e_i$ and $\hat{n}_{i,h} = h_i^\dagger h_i$. The model parameters are the nearest-neighbor E (H) hopping integral t_e (t_h), the energy of Einstein phonons ω_0 ($\hbar = 1$), the E (H)-phonon couplings α_e (α_h), as well as the local (extended) Coulomb interaction U_0 (U_1).

We consider a single E-H pair—a situation which can be studied experimentally³—and neglect X creation/recombination as well as dynamic screening of the Coulomb interaction due to other carriers or lattice polarization. Spin degrees of freedom are not taken into account, and we assume a tight-binding band structure with s symmetry for both E and H, neglecting the existence of a band gap (which here only leads to a shift of energies). Of course this

model is too simple to make a direct comparison with materials. Nevertheless, it does describe the physics of a Coulomb-bound, itinerant E-H pair whose constituents couple individually to quantum phonons and—in the absence of coupling to the lattice—captures the familiar crossover from a small to a large exciton with increasing bandwidth (see Sec. IV).¹⁸

The exact form of the carrier-phonon coupling is subject to X size, screening and material properties.⁸ We restrict our analysis to Holstein- and Fröhlich-type interactions well-known and understood from polaron physics, and amenable to efficient numerical treatment. Important aspects arise from the fact that the coupling of E and H to the lattice can either be of cooperative or compensating nature. The goal here is to obtain a qualitative understanding of the influence of the type and range of the lattice coupling, as well as the nonadiabaticity of the lattice.

Equation (1) allows for different signs of α_e and α_h . The coefficients $f_{j,i}$ correspond to a lattice version of the Fröhlich interaction with longitudinal optical phonons,²⁶ but yield a Holstein coupling to transverse optical phonons for $f_{j,i} = \delta_{i,j}$. Since E and H couple to the same phonon mode, we consider the symmetric mass case $t_e = t_h = t$, and $\alpha_h = \sigma\alpha_e = \sigma\alpha$ with $\sigma = \pm$ and $\alpha > 0$. We refer to the model with local respectively long-range carrier-lattice coupling as the Holstein-X model (HXM), respectively, Fröhlich-X model (FXM). These models capture the interplay of Coulomb attraction, particle motion and coupling to the lattice.

We introduce the dimensionless parameter $\lambda = 2\varepsilon_P(\sum_j f_{j,0}^2)/W$, where $\varepsilon_P = \alpha^2/2\omega_0$ is the polaron binding energy in the atomic limit and $W = 4t$ is the bare single-particle bandwidth. The time scales of E/H and quantum lattice dynamics are set by the adiabaticity ratio $\gamma = \omega_0/t$. The units of energy and length are taken to be U_0 and the lattice constant, respectively.

III. METHOD

The world-line QMC method adapted here can handle long-range interactions—notoriously difficult for many other numerical approaches—higher dimensions, and general fermion and phonon dispersion relations.^{27,28}

From the partition function with discretized inverse temperature $\beta = 1/(k_B T)$ and Trotter parameter $\Delta\tau = \beta/L$, the fermionic trace can be evaluated using real-space basis states $\{r_\tau^\rho\} = \{r_\tau^e, r_\tau^h\}$, which define world-line configurations on a $N \times L$ space-time grid. The path integral over the phonons is done analytically, yielding the fermionic partition function

$$Z_f = \sum_{\{r_\tau^\rho\}} e^{\sum_{\tau,\tau'} F(\tau-\tau')} \sum_{\rho,\rho'} \alpha_\rho \alpha_{\rho'} \phi(r_\tau^\rho - r_{\tau'}^{\rho'}) \quad (4)$$

$$\times e^{-\Delta\tau \sum_\tau u_{r_\tau^e, r_\tau^h}} \prod_\rho \prod_\tau I_\rho(r_{\tau+1}^\rho - r_\tau^\rho).$$

Here carrier-phonon coupling gives the memory function

$$F(\tau) = \frac{\omega_0 \Delta\tau^3}{4L} \sum_{\nu=0}^{L-1} \frac{\cos[2\pi\tau\nu/L]}{1 - \cos[2\pi\nu/L] + (\omega_0 \Delta\tau)^2/2} \quad (5)$$

with $\phi(r_\tau^\rho - r_{\tau'}^{\rho'}) = \sum_j f_{j,r_\tau^\rho} f_{j,r_{\tau'}^{\rho'}}$ and hopping enters via

$$I_\rho(r) = \frac{1}{N} \sum_{k=0}^{N-1} \cos(2\pi k r/N) e^{2\Delta\tau t_\rho \cos(2\pi k/N)}. \quad (6)$$

We calculate the X “radius” (see Ref. 17)

$$R = \left\langle \sum_{i,j} (i-j)^2 \hat{n}_{i,e} \hat{n}_{j,h} \right\rangle^{1/2}, \quad (7)$$

the kinetic energy

$$E_{\text{kin}} = -t \left\langle \sum_{(i,j)} e_i^\dagger e_j + h_i^\dagger h_j \right\rangle, \quad (8)$$

and the binding energies

$$E_{B,U} = E_X(t, U_0, U_1, \lambda) - 2E_e(t, \lambda) \quad (9)$$

and

$$E_{B,\lambda} = E_X(t, U_0, U_1, \lambda) - E_X(t, U_0, U_1, 0), \quad (10)$$

where E_X (E_e) denotes the X (E) energy. We further study the E-H correlation function

$$C_{eh}(r) = \sum_i \langle \hat{n}_{i,e} \hat{n}_{i+r,h} \rangle, \quad (11)$$

and the E-phonon correlation function

$$C_{eph}(r) = \sum_i \langle \hat{n}_{i,e} \hat{x}_{i+r} \rangle. \quad (12)$$

Computer time $\sim (\beta/\Delta\tau)^2$ (Ref. 27) sets a practical lower limit on simulation temperatures. The Trotter error (which can be removed by scaling to $\Delta\tau = 0$, see Ref. 29) and statistical errors limit the accuracy of our QMC results to typically 1%, and we use periodic clusters with $N = 32$. More sophisticated QMC approaches to polaron problems, free of Trotter errors and finite-size effects,^{30,31,32} have been developed. Whereas the continuous-time method has recently been applied to a similar model,³³ an extension of the diagrammatic MC method^{18,34} to the exciton-polaron problem is not yet available. Since all three methods are useful only for one or two carriers coupled to phonons and hence not applicable to more realistic systems, we have chosen the simplest approach currently available.

IV. RESULTS

To set the stage for the following discussion of lattice effects, and to demonstrate that the model defined by Eq. (1) describes the basic exciton physics, we begin with the case $\lambda = 0$, i.e., no coupling to the lattice. Figure 1 shows exact diagonalization (ED) and QMC results for the X size versus bandwidth. The zero-temperature ED data for $N = 31$ is well

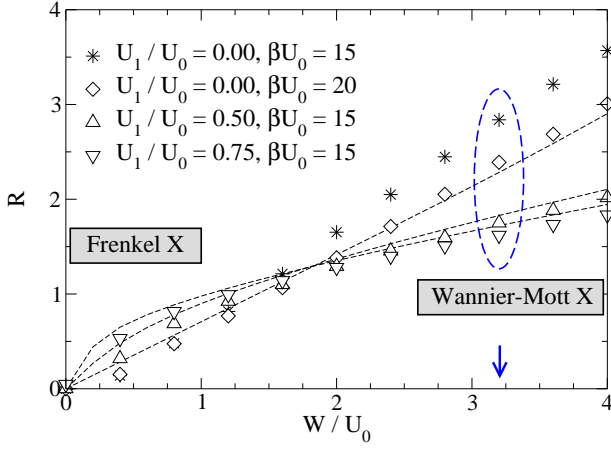


FIG. 1: Exciton radius R as a function of bandwidth W for $\lambda = 0$ and different values of U_1 . Dashed lines correspond to exact ground-state results ($N = 31$). QMC error bars are smaller than the symbols.

converged with respect to system size. With increasing W , there is a crossover from a small, strongly bound Frenkel-X with $R \approx 0$ (i.e., E and H at the same site) to a larger Wannier-Mott-like X with $R > 1$. Note that the X is always bound in 1D.¹⁷ Our parameters do not include the extensively studied Wannier-Mott limit, but instead cover experimentally relevant intermediate radii.¹⁸ The crossover point ($W/U_0 \approx 2$) separates regions with opposite dependence of R on U_1 .¹⁷ The QMC results are overall in good agreement with $T = 0$ ED data, with finite-temperature effects being most noticeable for $U_1 = 0$.

In the sequel, we restrict ourselves to the wide-band case $W/U_0 = 3.2$, highlighted in Fig. 1, for which $R(\lambda = 0) \gtrsim 1$. As this work is concerned with phonon effects, we focus on the dependence on λ and γ , and only consider $U_1/U_0 = 0.75$ and $\beta U_0 = 15$.

Discussing carrier-quantum-phonon interaction, it is crucial to distinguish between $\sigma = +$ and $-$, as well as between the adiabatic (slow lattice, $\gamma \ll 1$) and the non-adiabatic (fast lattice, $\gamma \gg 1$) regime, taking $\gamma = 0.4$ respectively $\gamma = 4$. We begin with the HXM in the adiabatic regime and $\sigma = +$.

Figure 2(a) shows R as a function of λ . With increasing coupling, there is a gradual crossover to a small X-P due to the increasingly strong phonon-mediated attractive interaction between E and H. The E- and H-polarons tend to maximize both the Coulomb and the lattice energy by forming a state with small R , but compete with the kinetic energy of the system which decreases with increasing λ (Fig. 3). Similar to the bipolaron problem with $U = 0$, E- and H-polarons form a (phonon) bound state at any $\lambda > 0$ in 1D. Most notably, there is no discontinuity at a critical λ , a common misconception due to earlier variational treatments, as quantum lattice fluctuations give rise to a translational invariant Bloch-like X-P state.

The crossover is also reflected in a reduced X mobility, and in a more negative X binding energy [Fig. 4(a)]. With the present method, dynamic quantities such as the effective exciton mass cannot be accurately calculated. An alternative ob-

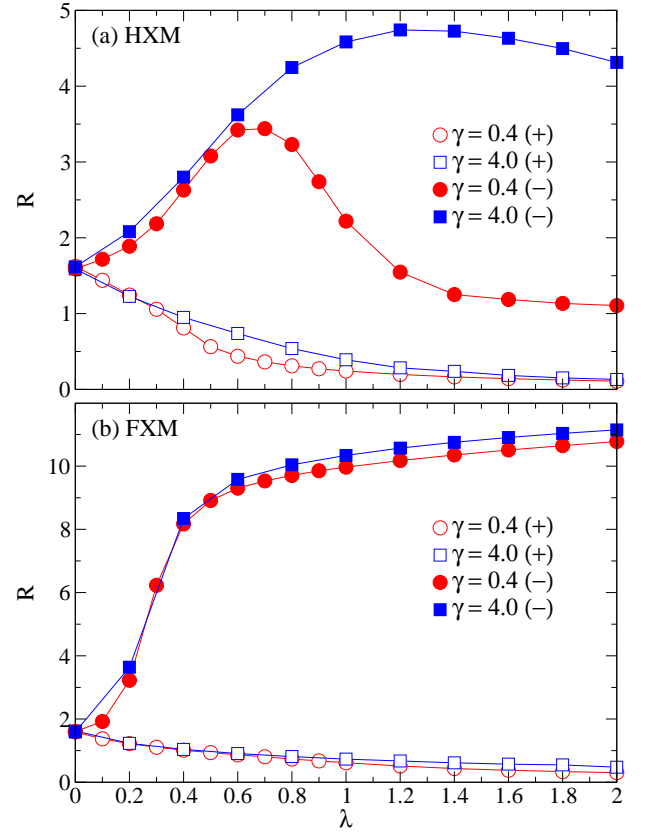


FIG. 2: (Color online) QMC results for R as a function of λ for (a) the HXM (see text) and (b) the FXM for both the adiabatic ($\gamma = 0.4$) and the nonadiabatic ($\gamma = 4$) regime, as well as $\sigma = \pm$. Here and in subsequent figures $\beta U_0 = 15$, $W/U_0 = 3.2$, $U_1/U_0 = 0.75$, and lines connecting data points are guides to the eye.

servable which to some degree (see, e.g., Ref. 35) measures the mobility is the kinetic energy shown in Fig. 3. In addition, the E-H and E-phonon correlation functions in Fig. 5(a), always positive for $\sigma = +$, fall off quickly with r , indicating that the X-P is a quasiparticle consisting of a tightly-bound E-H pair with a strongly localized surrounding lattice distortion. Such a state is similar to the Frenkel limit considered in Ref. 36.

The nonadiabatic regime $\gamma \gg 1$ mainly differs by a weaker dependence on λ (the important coupling parameter is ε_P/ω_0 , see below). The results for the FXM exhibit qualitatively the same tendencies, but the long-range interaction generally leads to larger E- and H-polarons and a larger X-P.

Turning to the case $\sigma = -$, we briefly discuss the different polaron ground states in the Holstein and the Fröhlich model. The Holstein model in 1D exhibits a crossover from a large polaron to a small polaron (with a predominantly onsite lattice distortion) with increasing λ . For $\gamma \ll 1$, the latter occurs near $\lambda \approx 1$, whereas for $\gamma \gg 1$ the condition is $\varepsilon_P/\omega_0 \gtrsim 1$ ($\lambda = 2$ for $\gamma = 4$).³⁶ In contrast, the Fröhlich polaron remains large (spatially extended lattice polarization) even for strong coupling.²⁶ While for $\sigma = +$ the bipolaron effect dominates, these differences have a major impact for $\sigma = -$ where

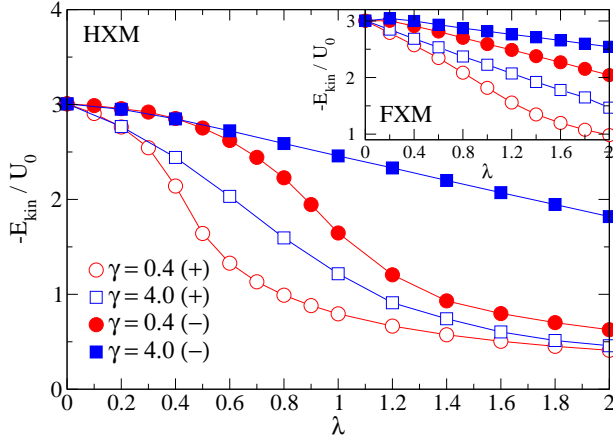


FIG. 3: (Color online) Kinetic energy E_{kin} .

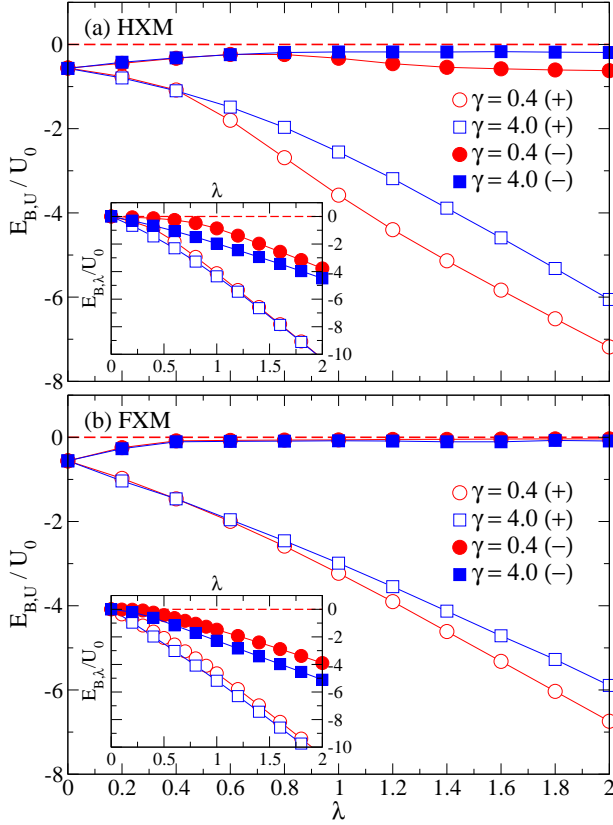


FIG. 4: (Color online) Binding energies $E_{B,U}$ and $E_{B,\lambda}$ (inset).

the Coulomb-bound E- and H-polarons remain separated with $R \gtrsim 1$.

In Fig. 2, strikingly different to $\sigma = +$, R initially increases with increasing λ , i.e., the X-P is larger for stronger coupling. In the HXM [Fig. 2(a)], R takes on a maximum at $\lambda \approx 0.7$ and approaches $R = 1$ for $\lambda \gtrsim 1$, whereas in the FXM R increases monotonically and saturates at large R in the strong-coupling regime [Fig. 2(b)]. Accordingly, the kinetic energy in Fig. 3 is much larger compared to $\sigma = +$, but is eventually reduced for large λ in the HXM. The binding energy $E_{B,U} \rightarrow 0$ with in-

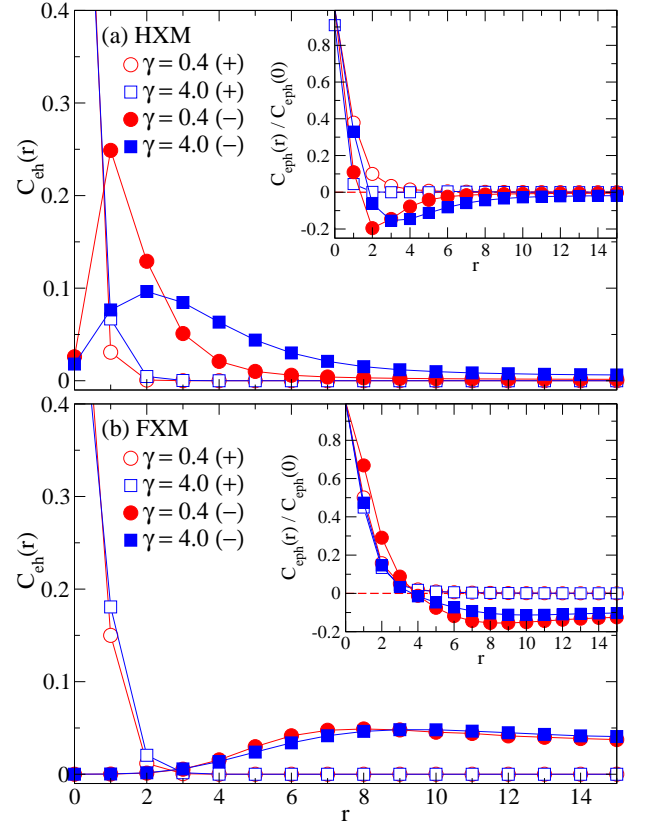


FIG. 5: (Color online) Electron-hole [$C_{eh}(r)$] and electron-phonon [$C_{eph}(r)$, inset] correlation functions for $\lambda = 1$.

creasing coupling in both models (Fig. 4), whereas $E_{B,\lambda}$ (see insets)—related to X-P effects—remains clearly negative.

The (initial) increase of the radius with increasing λ for the (HXM) FXM (Fig. 2) is due to the fact that the X-P loses lattice energy if the compensating displacement clouds surrounding E and H overlap. Therefore, the E- and H-polarons optimize R to achieve maximum Coulomb energy and minimum phonon-cloud overlap. The resulting average distance R depends on the size of the individual (E and H) polarons. For the HXM, polarons are large for $\lambda < 1$, leading to large values of R in Fig. 2(a), and become small for $\lambda > 1$, causing the decrease of $R \rightarrow 1$ in the strong-coupling regime. In the FXM, polarons remain large for all λ , leading to large values of R even for strong coupling [Fig. 2(b)]. The larger radius in the non-adiabatic HXM in Fig. 2(a) as compared to $\gamma \ll 1$ is due to the much larger polaron kinetic energy.³⁵ A discontinuous dissociation of the X-P with increasing λ has been discussed in a continuum model with acoustic phonons and $\sigma = -$.²¹

From the $\sigma = -$ results for the E-H correlation function in Fig. 5 we see that the E-H separation is small in the HXM, whereas the pair is spread out in the FXM. For the HXM with $\gamma = 0.4$, we find a charge-transfer X-P with E and H mainly on neighboring sites. Note that for $\sigma = -$, Coulomb and carrier-phonon interaction have swapped roles as compared to bipolaron formation where the lattice-coupling creates an attractive interaction that competes with Coulomb repulsion.³⁷

Turning to the E-phonon correlation functions in Fig. 5, we have $C_{eph} > 0$ for small r , but $C_{eph} < 0$ at larger distances as a result of the opposite distortions created by the hole. Again, the extent of the distortions is much larger for the FXM.

Real materials will require more detailed modeling, but we note that charge-transfer Xs in oxides will be better modeled by $\sigma = -$ (for breathing modes), whereas the characteristic case for a direct X in a neutral semiconductor would be $\sigma = +$.

V. CONCLUSIONS

In summary, we have studied the exciton-polaron problem with quantum phonons by Monte Carlo simulations. Our simple models encompass short- and long-range carrier-phonon interaction of either the same or opposite sign for electron and hole. There are no sharp transitions with increasing carrier-phonon coupling, and for couplings of opposite sign the exciton radius increases with increasing coupling as a result of polaron-polaron repulsion. To capture this effect (depending on polaron size which is affected by nonadiabaticity) relative

electron-hole motion and quantum phonon fluctuations must be taken into account. Our findings are expected to be important in materials with relatively small excitons such as organics and transition metal oxides, although more realistic models will have to be studied for direct comparison.

The present study motivates future work in a number of different directions, including more general models with respect to band structure, phonon dispersion, spin dependence, disorder, or dimensionality, and many-X-P as well as X-polariton problems. To this end, the development of more elaborate numerical approaches is highly desirable, permitting investigations of spectral properties routinely studied experimentally or even time-resolved studies of X formation.^{3,38}

Acknowledgments

This work was financially supported by the FWF Erwin Schrödinger Grant No. J2583 and the DFG through SFB 652. We thank A. Alvermann, P. Eastham, V. Heine, and F. Laquai for valuable discussions.

* Electronic address: mh507@cam.ac.uk

- ¹ I. Egri, Phys. Rep. **119**, 363 (1985).
- ² W. Barford, *Electronic and Optical Properties of Conjugated Polymers* (Oxford University Press, Oxford, 2005).
- ³ F. Dubin, R. Melet, T. Barisien, R. Grousson, L. Legrand, M. Schott, and V. Voliotis, Nat. Phys. **2**, 32 (2006).
- ⁴ A. J. Shields, Nat. Photonics **1**, 215 (2007).
- ⁵ J. Kasprzak, M. Richard, S. Kundermann, A. Baas, P. Jeambrun, J. M. J. Keeling, F. M. Marchetti, M. H. Szymanska, R. Andre, J. L. Staehli, V. Savona, P. B. Littlewood, B. Deveaud, and L. Dang, Nature (London) **443**, 409 (2006).
- ⁶ S. G. Chou, F. Plentz, J. Jiang, R. Saito, D. Nezich, H. B. Ribeiro, A. Jorio, M. A. Pimenta, G. G. Samsonidze, A. P. Santos, M. Zheng, G. B. Onoa, E. D. Semke, G. Dresselhaus, and M. S. Dresselhaus, Phys. Rev. Lett. **94**, 127402 (2005).
- ⁷ J. Frenkel, Phys. Rev. **37**, 17 (1931).
- ⁸ *Excitons*, edited by E. I. Rashba and M. D. Sturge (North-Holland Physics Publishing, Amsterdam, 1987), Vol. II, p. 543.
- ⁹ M. Gong, C.-F. Li, G. Chen, L. He, F. W. Sun, G.-C. Guo, Z.-C. Niu, S.-S. Huang, Y.-H. Xiong, and H.-Q. Ni, arXiv:0708.0468v2 (unpublished).
- ¹⁰ M. W. Kim, H. J. Lee, B. J. Yang, K. H. Kim, Y. Moritomo, J. Yu, and T. W. Noh, Phys. Rev. Lett. **98**, 187201 (2007).
- ¹¹ E. Collart, A. Shukla, J.-P. Rueff, P. Leininger, H. Ishii, I. Jarrige, Y. Q. Cai, S.-W. Cheong, and G. Dhalenne, Phys. Rev. Lett. **96**, 157004 (2006).
- ¹² J. Zaanen and P. B. Littlewood, Phys. Rev. B **50**, 7222 (1994).
- ¹³ K. M. Shen, F. Ronning, D. H. Lu, W. S. Lee, N. J. C. Ingle, W. Meevasana, F. Baumberger, A. Damascelli, N. P. Armitage, L. L. Miller, Y. Kohsaka, M. Azuma, M. Takano, H. Takagi, and Z.-X. Shen, Phys. Rev. Lett. **93**, 267002 (2004).
- ¹⁴ J.-F. Chang, J. Clark, N. Zhao, H. Sirringhaus, D. W. Breiby, J. W. Andreasen, M. M. Nielsen, M. Giles, M. Heeney, and I. McCulloch, Phys. Rev. B **74**, 115318 (2006).
- ¹⁵ H. Fehske, A. Alvermann, M. Hohenadler, and G. Wellein, in *Polarons in Bulk Materials and Systems with Reduced Dimensionality*, Proceedings of the International School of Physics “Enrico Fermi”, Course CLXI, edited by G. Iadonisi, J. Ranninger, and G. De Filippis (IOS Press, Amsterdam, 2006), pp. 285–296.
- ¹⁶ J. Ranninger, in *Polarons in Bulk Materials and Systems with Reduced Dimensionality*, Ref. 15, pp. 1–25.
- ¹⁷ K. Ishida, H. Aoki, and T. Chikyu, Phys. Rev. B **47**, 7594 (1993).
- ¹⁸ E. A. Burovski, A. S. Mishchenko, N. V. Prokof’ev, and B. V. Svistunov, Phys. Rev. Lett. **87**, 186402 (2001).
- ¹⁹ H. Haken, J. Phys. Chem. Solids **8**, 166 (1959).
- ²⁰ A. Suna, Phys. Rev. **135**, A111 (1964).
- ²¹ A. Sumi, J. Phys.: Condens. Matter **43**, 1286 (1977).
- ²² Y. Shinozuka and N. Ishida, J. Phys. Soc. Jpn. **64**, 3007 (1995).
- ²³ H. Sumi and A. Sumi, J. Phys. Soc. Jpn. **63**, 637 (1994).
- ²⁴ K. Ishida, Phys. Rev. B **49**, 5541 (1994).
- ²⁵ K. Ishida, Phys. Rev. B **55**, 12856 (1997).
- ²⁶ A. S. Alexandrov and P. E. Kornilovitch, Phys. Rev. Lett. **82**, 807 (1999).
- ²⁷ H. de Raedt and A. Lagendijk, Phys. Rep. **127**, 233 (1985).
- ²⁸ M. Hohenadler and P. B. Littlewood, Phys. Rev. B **76**, 155122 (2007).
- ²⁹ P. E. Kornilovitch, J. Phys.: Condens. Matter **9**, 10675 (1997).
- ³⁰ P. E. Kornilovitch, Phys. Rev. Lett. **81**, 5382 (1998).
- ³¹ P. E. Kornilovitch, Phys. Rev. B **60**, 3237 (1999).
- ³² N. V. Prokof’ev and B. V. Svistunov, Phys. Rev. Lett. **81**, 2514 (1998).
- ³³ J. P. Hague, P. E. Kornilovitch, J. H. Samson, and A. S. Alexandrov, Phys. Rev. Lett. **98**, 037002 (2007).
- ³⁴ A. Macridin, G. A. Sawatzky, and M. Jarrell, Phys. Rev. B **69**, 245111 (2004).
- ³⁵ J. Loos, M. Hohenadler, A. Alvermann, and H. Fehske, J. Phys.: Condens. Matter **19**, 236233 (2007).
- ³⁶ G. Wellein and H. Fehske, Phys. Rev. B **58**, 6208 (1998).
- ³⁷ M. Hohenadler and W. von der Linden, Phys. Rev. B **71**, 184309 (2005).

- ³⁸ J. Edler, P. Hamm, and A. C. Scott, Phys. Rev. Lett. **88**, 067403 (2002).